Research Article Vol. 3, No. 12 / 15 December 2020 / OSA Continuum 3574


# Generation of visible-wavelength-tunable ultrashort laser pulses through femtosecond laser filamentation in air: strong external focusing effect

YAN ZHOU,[1,5] NANA DONG,[1,5] SHANBIAO PANG,[1] HANXIAO LI,[1] LUNHUA DENG,[1,6] JIAN WU,[1] AND HUAILIANG XU[1,2,3,4,7]

[1]State Key Laboratory of Precision Spectroscopy, East China Normal University, Shanghai 200062, China
[2]State Key Laboratory of Integrated Optoelectronics, College of Electronic Science and Engineering, Jilin University, Changchun 130012, China
[3]CAS Center for Excellence in Ultra-Intense Laser Science, Shanghai 201800, China
[4]Chongqing Institute of East China Normal University, Chongqing 401120, China
[5]These authors contributed equally to this work.
[6]lhdeng@phy.ecnu.edu.cn
[7]huailiang@jlu.edu.cn

**Abstract:** Wavelength-tunable ultrashort laser pulses in the visible spectral range are generated in a femtosecond laser filament in air through four-wave mixing of an intense 808-nm near-infrared (NIR) laser pulse and a weak tunable infrared (IR: 1.3–2.2 μm) laser pulse. We found that the external focusing geometries strongly influence the four-wave mixing efficiency in air filament. The measurements of the resultant four-wave mixing laser intensity reveal that changing both the tilting angle and the focal length of the focal lens can optimize the four-wave mixing signal. We interpret the process based on the strong influence of the external focusing on the plasma density and the volume of the filament during the filament formation.



## 1. Introduction

Nowadays, intense wavelength-tunable ultrashort lasers play a significant role in many fundamental research fields and applications such as atomic and molecular spectroscopy, chemical reactions, and biological processes. A variety of methods have been developed so far to produce tunable ultrashort pulses in the infrared (IR), visible and ultraviolet (UV) ranges, among which the nonlinear frequency conversion techniques such as optical parametric amplification [1] and four-wave mixing [2] are the most attractive ones. In particular, for the direct generation of shorter wavelength laser than that of the pump laser, four-wave mixing is a powerful and promising method, which generally requires the nonlinear media having a large third-order nonlinear coefficient $\chi^{(3)}$ to improve the conversion efficiency. Therefore, solid media with large $\chi^{(3)}$ have often been explored to produce tunable visible and UV ultrashort pulses using various four-wave mixing schemes [3–7]. However, solid media suffer optical damage at high pump laser intensities, which severely limits their application in producing high-power four-wave mixing lasers. Besides, the limited optical transparency region of some specific solid media restricts the tunable spectral ranges of the resultant four-wave mixing pulses.

On the other hand, gas media are suitable for nonlinear frequency conversion processes driven by an intense laser field due to their high damage threshold under optical excitation. Consequently, many efforts have been made to develop ultrashort intense four-wave mixing pulses in various gases with the operation wavelengths over a wide spectral range [8,9]. More interestingly, it was demonstrated that a highly efficiently four-wave mixing process can occur in a femtosecond laser filament, producing ultrashort tunable laser pulses with very low energy fluctuation and excellent

#406120 https://doi.org/10.1364/OSAC.406120
Journal © 2020 Received 24 Aug 2020; revised 3 Dec 2020; accepted 4 Dec 2020; published 14 Dec 2020

OSA CONTINUUM

mode quality, which has been ascribed to the unique properties of the intensity clamping and self-filtering in the filament [10]. Also, due to the self-compression effect in the filament, the pulse duration of the resultant visible four-wave mixing pulses can be shortened to a few cycles, even to the single-cycle limit [11]. Moreover, it was demonstrated that the phase-synchronism effect on the four-wave mixing light in a filament is not very important [12]. Due to the benefit of four-wave mixing in the filament for producing ultrashort pulse, it has attracted considerable attention in recent years [11,13–18]. However, filamentation is a result of the dynamical balance between self-focusing and defocusing of air plasma [19], in which the clamping intensity and plasma density are strongly dependent on the external focusing conditions [20,21]. Indeed, the filamentation of high-power femtosecond laser pulses in air was experimentally and theoretically studied under conditions of a variety of the beam focusing parameters [22,23]. In addition, the spectral and spatial characteristics of infrared femtosecond laser pulses under tight focus was revealed [24]. These previous studies clearly showed that external focusing plays an essential role in the filament formation. Therefore, it is naturally questioned whether the four-wave mixing process in the filament would also be influenced by external focusing, which remains unclear until now.

In the present study, we generated wavelength-tunable ultrashort laser pulses in the visible spectral range in a femtosecond laser filament in air through four-wave mixing of an intense 808-nm near-infrared (NIR) laser pulse and a weak tunable IR laser pulse. We investigated the four-wave mixing pulse generation in the parameter space of external focusing geometries, including the focal length and tilt angle of the focal lens, incident pulse energy, as well as polarization, based on which we identify the optimization condition for the four-wave mixing pulse generation. We explain the optimal focusing condition of the four-wave mixing pulse generation on the basis of the understanding of the strong dependence of the external focusing on the plasma density and volume of the filament during the filament formation.

## 2. Experimental setup

The experiments were conducted using a Ti:Sapphire chirped-pulse amplification laser system (Coherent Inc. Astrella), which produced 35 fs laser pulses centering at 808 nm with a maximal pulse energy of 7 mJ and a repetition rate of 1 kHz. The experimental setup for the generation and optimization of the tunable visible four-wave mixing pulses is shown in Fig. 1. First, the fundamental NIR laser beam was split into two arms by a beam splitter with an energy ratio of 2:8. A less energetic NIR pulse was used to pump an optical parametric amplifier (OPA: Coherent OPerA-Solo), which produced tunable IR laser pulses in the wavelength range of 1.14 –1.6 μm (Signal) and 1.6 –2.6 μm (Idler), respectively. The IR laser pulse was then attenuated with a gradient neutral density filter. The more energetic NIR pulse beam was controlled using a half-wave plate and a polarizing beam splitter. Then a dichroic mirror was used to overlap the NIR and IR laser pulses spatially. These two-color pulses propagated collinearly and were focused in the air by a focal lens. During the experiments, the spatial overlapping of the two beams was carefully examined to minimize its influence on the four-wave mixing generation. An optical delay line was inserted in the more energetic NIR optical path to adjust the temporal delay between the IR and NIR laser pulses.

After the focal lens, a filament was formed by the NIR pulse, which can be clearly seen from the side of the filament by naked eyes through observing the nitrogen fluorescence. Inside the filament core, the four-wave mixing process occurred through the strong nonlinear interaction between the IR laser pulse and the NIR fundamental pulse during their co-propagation. After the filament, the NIR and IR pump pulses and the resultant four-wave mixing pulse were first reflected by an N-BK7 window so that only 8% of the four-wave mixing pulse remained to be detected. Then the NIR and IR pulses were filtered out with a low pass filter (< 600 nm pass)

OSA CONTINUUM

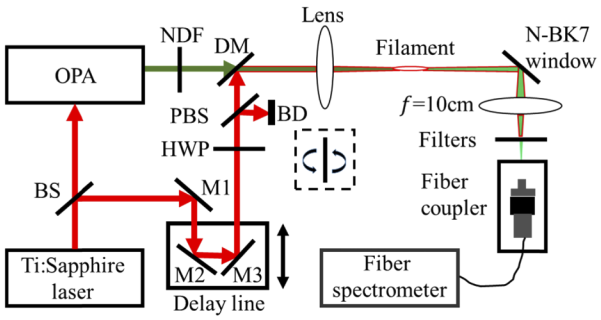


**Fig. 1.** Four-wave mixing generation using a femtosecond Ti:Sapphire laser and an ultrafast optical parametric amplifier (OPA) laser. BS: beam splitter; M1-M3: mirrors; HWP: half-wave plate; PBS: polarizing beam splitter; BD: beam dump 808 nm; NDF: neutral density filter; DM: dichroic mirror.

and a bandpass filter plate (350–700 nm pass), and the transmitted four-wave mixing pulse was collected with a spectrometer using a focus lens.

## 3. Result and discussion

### *3.1. Generation of tunable four-wave mixing pulses*

Figure 2(a) shows the forward four-wave mixing laser patterns and their corresponding spectra obtained by tuning the IR pulse from 1.3 - 2.2 μm. The frequencies of the generated four-wave mixing pulses, $\omega_{FWM}$, satisfy the relation of $\omega_{FWM} = 2\omega_{NIR} - \omega_{IR}$, where $\omega_{NIR}$ and $\omega_{IR}$ represent the frequencies of the NIR and IR pulses, respectively. In this measurement, the incident powers of NIR and IR were about 0.60 mJ/pulse and 0.12 mJ/pulse, respectively, and the focal length of the lens was 75 cm. In this case, the strong NIR pulse was used to generate a single filament in air, and the weak IR pulse (0.12 mJ) was adopted to stimulate the four-wave mixing in the filament. A digital camera was used to take the photos of the four-wave mixing beam pattern, which was imaged on a white paper using a concave mirror. As shown in Fig. 2(a), the generated four-wave mixing pulses have the Gaussian-shaped distribution with the central wavelengths in the range of 488–569 nm and the bandwidth in the range of 13 nm to 30 nm (the full width at half-maximum). It should be emphasized that the wavelength tuning range and spectral line shape are in good agreement with the previous studies [10].

Since the polarization matching of NIR and IR light pulses is essential for the four-wave mixing process, we measured the generated four-wave mixing pulse intensity as a function of the angle between the polarization directions of the NIR and IR pulses. In the measurement, the incident energies of NIR (808 nm) and Idler IR (1.9 μm) were 0.50 mJ/pulse and 0.11 mJ/pulse, respectively. The NIR and IR pulses were linearly polarized with the polarization directions of both the NIR and Idler pulses being horizontal. A half-wave plate was used to adjust the polarization direction of the NIR laser with respect to that of the IR laser. The reflected power of the NIR laser did not change much with the rotation of the half-wave plate. As shown in Fig. 2(b), when the polarization direction of the NIR laser is parallel to that of the IR laser, the intensity (the peak value of the spectrum) of the four-wave mixing pulse reaches the maximum. When the polarization directions of the two incident pulses deviate from parallel, the intensity of the four-wave mixing pulse decreases monotonically and reaches a minimum when the polarization of the two pulses are perpendicular.

As illustrated above, we have clearly generated wavelength-tunable ultrashort laser pulses in the air filament through four-wave mixing with the wide tunable range in the visible spectral

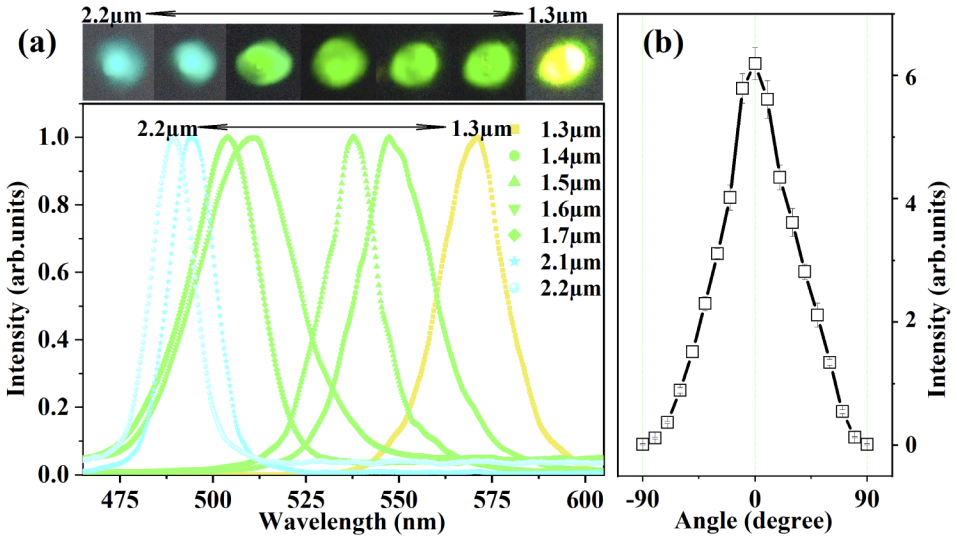


**Fig. 2.** (a) Patterns of the generated four-wave mixing laser pulses and the corresponding normalized spectra. The IR laser wavelength is tuned from 2.2 μm to 1.3 μm, and the four-wave mixing pulse wavelength changes from 488 nm to 569 nm. (b) The measured spectral intensity of the four-wave mixing pulse as a function of the angle between the polarization directions of incident NIR and IR light pulses. The zero degree means that the polarization directions of the NIR and IR lasers are parallel.

region. In the following sections, we will investigate the influence of external focusing geometries and incident light power on the four-wave mixing signal, and attempt to identify the optimization condition for the four-wave mixing pulse generation in the air filament.

### *3.2. Effect of focal length on the four-wave mixing signal*

The focal length could be one of the most critical parameters that can influence the conversion efficiency of four-wave mixing since the clamping intensity and plasma density in the filament strongly depend on the external focusing [21]. In this measurement, we recorded the spectral intensity of the four-wave mixing signal at different focal lengths by keeping other settings unchanged. The incident powers of the NIR and IR laser pulses were 0.60 mJ/pulse and 0.12 mJ/pulse, respectively. The IR wavelength was set at 2.0 μm, and the center wavelength of the produced four-wave mixing pulse was centered at 505 nm. Figure 3 shows the peak intensity of the four-wave mixing pulses obtained at different focal lengths. It can be seen that the peak intensity of the four-wave mixing signal increases slowly with the increase of the focal length, and reaches the maximum when the focal length is 75 cm, and then decreases.

It was previously demonstrated that under the short focal length conditions, a tight focusing causes high plasma density and small filament volume; while as the focal length increases, the plasma density becomes smaller, and the filament diameter increases, and then slightly decreases [21], which is in a good agreement with our measurement (not shown). Since the plasma produced by a laser pulse causes pulse intensity clamping at some quasi-constant level, the high plasma density limits the four-wave mixing signal. With the increase of the filament diameter and length, the interaction volume of the NIR and IR pulses also increases, which will benefit the generation of the four-wave mixing signal. Therefore, as the focal length increases from 10 cm to 75 cm, the intensity of the four-wave mixing signal increases. When the focal length reaches 75 cm, the influence of the interaction volume and the plasma density reaches an equilibrium, and the four-wave mixing signal reaches the maximum.

OSA CONTINUUM

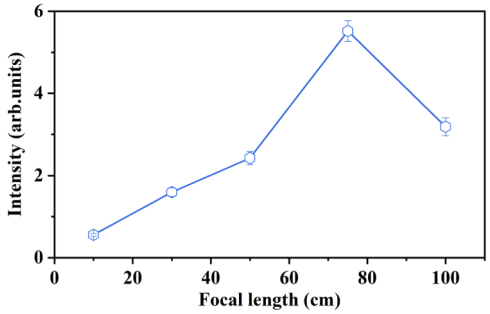


**Fig. 3.** The intensities of the four-wave mixing pulses were measured with different focal lengths.

However, when the focal length continues to increase, the intensity of the four-wave mixing signal decreases. At the loosely focusing condition, one reason for the decrease in the four-wave mixing signal is the filament length saturation for high numerical aperture values of the laser beam [23]. Another reason may be that the plasma density, and also the clamping intensity decrease significantly as the focal length increases [20], which decreases the nonlinear interaction strength, and thus reduces the four-wave mixing signal. Moreover, although the filament volume continues to increase with the focal length, the longer filament may lead to a poor phase-matching for the decrease in the four-wave mixing signal [11]. As a consequence, the four-wave mixing generation in a filament depends on a few parameters including the plasma density, filament volume, phase-matching and laser intensity.

### *3.3. Effect of lens tilting on the four-wave mixing signal*

Previous studies have shown that lens tilting can control the number, pattern, spatial stability of filaments, and enhance the signal-to-noise ratio of filament induced fluorescence [25–27]. However, the effect of lens tilting on the four-wave mixing signal has not been investigated. Here we studied the impact of lens tilting on the four-wave mixing signal. The focusing lens was placed on a horizontal rotating table, which drives the lens to rotate along the vertical axis, thus changing the angle between the incident light pulses and the lens. Figure 4 shows the peak

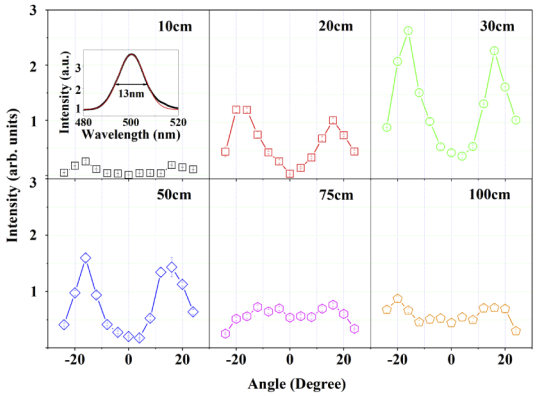


**Fig. 4.** The intensity of the four-wave mixing signal varies with the tilt angle at different focal lengths. The inset shows the spectrum obtained with a 10 cm lens at a tilt angle of 16 degrees and the Gaussian fitting profile of the spectrum, giving a full width at half maximum of 13 nm.

OSA CONTINUUM

four-wave mixing spectral intensity as a function of the tilt angle at different focal lengths in the range of 10 to 100 cm. For clarity, the angle at which the lens rotates in one direction is marked as a negative value, and the opposite direction is marked as a positive value. The incident powers were 0.62 mJ/pulse and 0.11 mJ/pulse for NIR and IR (2.0 μm), respectively. One of the spectra and it's Gaussian fitting is shown in the first inset panel of Fig. 4, giving a bandwidth of 13 nm.

As shown in Fig. 4, for all the cases of the focal lengths used in this study, the four-wave mixing intensity varies with the tilt angle and has two maximum values, which are symmetrical to the normal incidence. That is, when the lens is rotated in any direction along the vertical axis, the four-wave mixing intensity will first increase and then decrease as the tilt angle increases. It is believed that this phenomenon is also affected by the plasma density and the filament volume. When the incident light pulse deviates from the normal incidence, the filament will split into two parts [27], and the overlap volume of the NIR and IR light pulses in the filament increases. The increase in overlap volume is the main reason why the intensity of the four four-wave mixing signal first increases with the increase in the tilt angle. However, when the tilt angle is too large, it will result in a much weaker plasma density and also poor phase matching due to the longer plasma length, making the four-wave mixing signal smaller. The optimal angle depends on the combined effect of the plasma density and the filament volume.

Another noteworthy phenomenon is that when the focal length is small, i.e., from 10 cm to 50 cm in Fig. 4, the intensity of the four-wave mixing signal changes significantly with the tilt angle. The reason is that there is a tight focusing under shorter focal length, and the filament volume varies considerably with the tilt angle. The change of the filament volume with the tilt angle causes the change of the four-wave mixing signal. When the focal length is long, i.e., 75 cm and 100 cm in Fig. 4, the change of intensity with the angle still exists, but the amplitude change is much smaller. At the longer focal length, the filament length and plasma density would not change much as the tilting angle changes [27], and thus the signal intensity does not change much with the change of the tilting angle of the lens.

### 3.4. *Effect of incident power on the four-wave mixing signal*

Since the incident light power affects the plasma density and the filament volume [21], it is expected that the incident power will also influence the intensity of the four-wave mixing signal. In Fig. 5, we show the measured peak spectral intensity of the four-wave mixing pulse as a function of $P/P_{cr}$ at different IR wavelengths, where P is the incident NIR power and $P_{cr}$ is the critical power. $P_{cr}$ is one of the essential parameters in the filament, and the value of $P_{cr}$ in this study is about 10 GW [28]. In this measurement, the IR energy was fixed at 0.12 mJ/pulse. The experiment used a lens with a focal length of 75 cm to focus the laser pulses under normal incidence. It can be seen from Fig. 5 that the four-wave mixing intensity increases first, and then as the power is above 3.5 $P_{cr}$, it is saturated for all the cases. Previous studies have shown

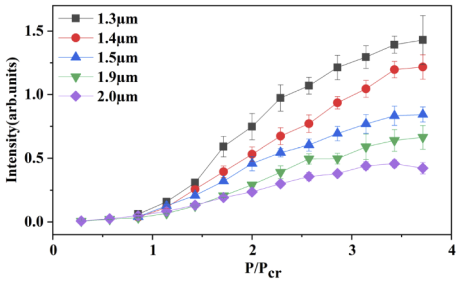


**Fig. 5.** The influence of NIR laser power on the peak spectral intensity of four-wave mixing at different IR wavelengths.

OSA CONTINUUM

that as $P/P_{cr}$ is small, the plasma density and filament diameter increase as the incident power, P, increases [21,29], but as $P/P_{cr}$ is larger than 3–3.5 [21], the plasma diameter and density are almost kept to be constant. Thus the results are shown in Fig. 5 can also be understood based on the variations of the plasma density and filament diameter, which results in a saturation of the four-wave mixing signal as $P/P_{cr}$ is larger than 3.5.

## 4. Summary

In summary, we have achieved the generation of wavelength-tunable visible ultrashort laser pulses in the air filament through the four-wave mixing, $\omega_{FWM} = 2\omega_{NIR} - \omega_{IR}$, of the NIR laser pulse at 808 nm and the tunable IR laser pulse at 1.3–2.2 μm. We have revealed that the four-wave mixing efficiency in the filament is strongly influenced by the external focusing geometries, including the focal length and tilt angle of the focal lens, and that the spectral intensity of the four-wave mixing signal is suffering a saturation at high incident power. These experimental results have been well explained based on the changes in the plasma density and volume in the filament under different experimental parameters. Our results may be useful for the optimization of four-wave mixing in femtosecond laser filament for visible and UV ultrashort laser pulse generation.

## Funding

National Natural Science Foundation of China (61625501); State Key Laboratory of High Field Laser Physics; Program for Jilin University Science and Technology Innovative Research Team (2017TD-21); Fundamental Research Funds for the Central Universities.

## Acknowledgments

We acknowledge the fruitful discussion with Andrius Baltuška from Vienna University of Technology, Austria.

## Disclosures

The authors declare no conflicts of interest.

## References

1. C. Manzoni and G. Cerullo, "Design criteria for ultrafast optical parametric amplifiers," J. Opt. **18**(10), 103501 (2016).
2. T. Kobayashi, J. Liu, and Y. Kida, "Generation and Optimization of Femtosecond Pulses by Four-Wave Mixing Process," IEEE J. Sel. Top. Quantum Electron. **18**(1), 54–65 (2012).
3. H. Crespo, J. T. Mendonca, and A. D. Santos, "Cascaded highly nondegenerate four-wave-mixing phenomenon in transparent isotropic condensed media," Opt. Lett. **25**(11), 829–831 (2000).
4. J. Liu and T. Kobayashi, "Cascaded four-wave mixing and multicolored arrays generation in a sapphire plate by using two crossing beams of femtosecond laser," Opt. Express **16**(26), 22119–22125 (2008).
5. R. V. Volkov, D. V. Khakhulin, and A. B. Savel'ev, "Four-wave parametric conversion of femtosecond laser pulse in a filament induced in a solid target," Opt. Lett. **33**(7), 666–668 (2008).
6. J. Liu and T. Kobayashi, "Wavelength-tunable, multicolored femtosecond-laser pulse generation in fused-silica glass," Opt. Lett. **34**(7), 1066–1068 (2009).
7. J. Liu, T. Kobayashi, and Z. Wang, "Generation of broadband two-dimensional multicolored arrays in a sapphire plate," Opt. Express **17**(11), 9226–9234 (2009).
8. L. Misoguti, S. Backus, C. G. Durfee, R. Bartels, M. M. Murnane, and H. C. Kapteyn, "Generation of broadband VUV light using third-order cascaded processes," Phys. Rev. Lett. **87**(1), 013601 (2001).
9. A. G. Ciriolo, A. Pusala, M. Negro, M. Devetta, D. Faccialà, G. Mariani, C. Vozzi, and S. Salvatore, "Generation of ultrashort pulses by four wave mixing in a gas-filled hollow core fiber," J. Opt. **20**(12), 125503 (2018).
10. F. Théberge, N. Aközbek, W. Liu, A. Becker, and S. L. Chin, "Tunable ultrashort laser pulses generated through filamentation in gases," Phys. Rev. Lett. **97**(2), 023904 (2006).
11. T. Fuji and T. Suzuki, "Generation of sub-two-cycle mid-infrared pulses by four-wave mixing through filamentation in air," Opt. Lett. **32**(22), 3330–3332 (2007).
12. V. A. Andreeva, N. A. Panov, O. G. Kosareva, and S. L. Chin, "Single-cycle pulse generation in the course of four-wave mixing in the filament," Proc. SPIE Int. Soc. Opt. Eng. **8512**, 85120Z (2012).

OSA CONTINUUM


13. F. Théberge, M. Châteauneuf, G. Roy, P. Mathieu, and J. Dubois, "Generation of tunable and broadband far-infrared laser pulses during two-color filamentation," Phys. Rev. A **81**(3), 033821 (2010).
14. M. Ghotbi, M. Beutler, and F. Noack, "Generation of 25 μJ vacuum ultraviolet pulses with sub-50 fs duration by noncollinear four wave mixing in argon," Opt. Lett. **35**(20), 3492–3494 (2010).
15. T. Horio, R. Spesyvtsev, and T. Suzuki, "Generation of sub-17fs vacuum ultraviolet pulses at 133 nm using cascaded four-wave mixing through filamentation in Ne," Opt. Lett. **39**(20), 6021–6024 (2014).
16. P. Zuo, T. Fuji, and T. Suzuki, "Spectral phase transfer to ultrashort UV pulses through four-wave mixing," Opt. Express **18**(15), 16183–16192 (2010).
17. M. Beutler, M. Ghotbi, F. Noack, and I. V. Hertel, "Generation of sub-50-fs vacuum ultraviolet pulses by four-wave mixing in argon," Opt. Lett. **35**(9), 1491–1493 (2010).
18. T. Fuji, T. Horio, and T. Suzuki, "Generation of 12 fs deep-ultraviolet pulses by four-wave mixing through filamentation in neon gas," Opt. Lett. **32**(17), 2481–2483 (2007).
19. A. Couairon and A. Mysyrowicz, "Femtosecond filamentation in transparent media," Phys. Rep. **441**(2-4), 47–189 (2007).
20. X. L. Liu, W. B. Cheng, M. Petrarca, and P. Polynkin, "Measurements of fluence profiles in femtosecond laser filaments in air," Opt. Lett. **41**(20), 4751–4754 (2016).
21. F. Théberge, W. Liu, P. T. Simard, A. Becker, and S. L. Chin, "Plasma density inside a femtosecond laser filament in air: Strong dependence on external focusing," Phys. Rev. E **74**(3), 036406 (2006).
22. Y. E. Geints, A. A. Zemlyanov, A. A. Ionin, S. I. Kudryashov, L. V. Seleznev, D. V. Sinitsyn, and E. S. Sunchugasheva, "Peculiarities of Filamentation of Sharply Focused Ultrashort Laser Pulses in Air," J. Exp. Theor. Phys. **111**(5), 724–730 (2010).
23. Y. E. Geints and A. A. Zemlyanov, "Self-focusing of a focused femtosecond laser pulse in air," Appl. Phys. B **101**(4), 735–742 (2010).
24. V. Vaicaitis, M. Kretschmar, R. Butkus, R. Grigonis, U. Morgner, and I. Babushkin, "Spectral broadening and conical emission of near-infrared femtosecond laser pulses in air," J. Phys. B: At., Mol. Opt. Phys. **51**(4), 045402 (2018).
25. S. Eisenmann, E. Louzon, Y. Katzir, T. Palchan, A. Zigler, Y. Sivan, and G. Fibich, "Control of the filamentation distance and pattern in long-range atmospheric propagation," Opt. Express **15**(6), 2779–2784 (2007).
26. G. Fibich, S. Eisenmann, B. Ilan, and A. Zigler, "Control of multiple filamentation in air," Opt. Lett. **29**(15), 1772–1774 (2004).
27. Y. Kamali, Q. Sun, J.-F. Daigle, A. Azarm, J. Bernhardt, and S. L. Chin, "Lens tilting effect on filamentation and filament-induced fluorescence," Opt. Commun. **282**(5), 950–954 (2009).
28. W. Liu and S. L. Chin, "Direct measurement of the critical power of femtosecond Ti : sapphire laser pulse in air," Opt. Express **13**(15), 5750–5755 (2005).
29. Y. P. Deng, J. B. Zhu, Z. G. Ji, J. S. Liu, B. Shuai, R. X. Li, Z. Z. Xu, F. Theberge, and S. L. Chin, "Transverse evolution of a plasma channel in air induced by a femtosecond laser," Opt. Lett. **31**(4), 546–548 (2006).